Advanced Composite Materials
Publication details, including instructions for authors and subscription information:
http://www.tandfonline.com/loi/tacm20

Anisotropic transparency of polystyrene film with crazes

Akiyoshi Takeno [a], Norikazu Nakagaki [b] & Minoru Miwa [c]
[a] Department of Chemistry, Faculty of Engineering, Gifu University, 1-1 Yanagido, Gifu 501-11, Japan
[b] Department of Chemistry, Faculty of Engineering, Gifu University, 1-1 Yanagido, Gifu 501-11, Japan
[c] Department of Chemistry, Faculty of Engineering, Gifu University, 1-1 Yanagido, Gifu 501-11, Japan
Version of record first published: 02 Apr 2012.

To cite this article: Akiyoshi Takeno, Norikazu Nakagaki & Minoru Miwa (1998): Anisotropic transparency of polystyrene film with crazes, Advanced Composite Materials, 7:1, 35-46

To link to this article: http://dx.doi.org/10.1163/156855198X00039

Adv. Composite Mater., Vol. 7, No. 1, pp. 35–46 (1998)

Anisotropic transparency of polystyrene film with crazes

AKIYOSHI TAKENO,* NORIKAZU NAKAGAKI and MINORU MIWA

Department of Chemistry, Faculty of Engineering, Gifu University, 1-1 Yanagido, Gifu 501-11, Japan

Received 27 September 1996; accepted 27 December 1996

Abstract—A crazing method was developed to create regular crazes in a polystyrene film. The crazes penetrated completely in the direction of film thickness. The tensile strength of the crazed films in both perpendicular and parallel directions to the processing direction was almost unchanged after the crazing-processing, regardless of crazing conditions. Young's modulus in the parallel direction decreased with the film tension during the crazing-processing. If suitable crazing-processing was used, transmittance of incident light decreased between the incident angles of 0 to 20 deg, and increased above the angle of *ca* 20 deg with an increasing incident angle, which gives a W-shape to the light transmittance curve.

Keywords: Craze; anisotropy; transparency; polystyrene; crazing-processing; mono-component composites; view control film.

1. INTRODUCTION

View-field selectability that can control the field of view through the viewing angle has been investigated, because of problems such as interference of sunlight with displays for automobiles and aircraft and protection of privacy in housing. These selectable glasses and films have been manufactured by stripe printing, multiple layer film and blended film which has consisted of two different index phases by UV polymerization [1].

We have reported on the mechanical properties of poly(vinylidene fluoride) (PVDF) with regular crazes [2]. The film consists of craze and non-craze layers and shows anisotropy in Young's modulus in the directions perpendicular and parallel to the crazing-processing, accompanied with sharp-edged bending as mentioned later. This crazing PVDF film displayed a transparency film in normal direction to the film surface and an opaque film at the tilt of the view point, because the scattering property of incident light depends on the incident angle. The craze layers in the film are similar to the slat of a blind [2–4]. This film is considered to be useful view-field selectable film.

*To whom correspondence should be addressed.

PVDF films are expensive and view-field selectable film is not only the transparency film in front but also the opaque film in front which will be required. In this paper we have explored mechanical and optical properties of polystyrene (PS) film treated by a unique crazing-processing which had angular dependence of transparency different from crazed PVDF films. A characteristic crazing morphology and transmittance curve according to the angle of incident light were investigated.

2. EXPERIMENTAL

2.1. Test materials

High impact resistant type PS films (Harlen L, Toyo Chem. Co., thickness 25 μm, including styrene–butadiene (SBS) copolymer) were used. The PS : SBS composition was 70 : 30. SBS particles disperse finely (diameter below 0.1 μm) and uniformly in the PS matrix and the films have high transparency for optical applications.

2.2. Crazing-processing

The crazing-processing used in this study is shown in Fig. 1, and is essentially the same as that used in a previous paper [2]. The crazing device was mounted on a tensile tester (Orientec Co., Tensilon UTM-I/2500). The film (50 × 300 mm) was bent sharply at the crazing-edge (Fig. 1) under a constant tension. The pulling tension (1, 2, 4, 6 and 8 N/cm) was controlled by the friction resistance of a revolving roller (the tension roller in Fig. 1). The pulling rate of the crazing-processing is equal to the cross head speed of the tensile tester and controlled at 10, 20, 30, 50 and 100 mm/min, respectively. The bending angle of the film at the crazing edge was kept at *ca* 145 deg. The radius of the tip of the crazing-edge was *ca* 50 μm. The

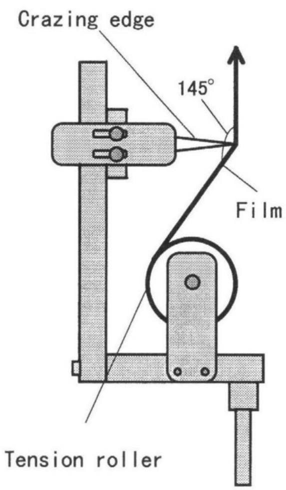

Figure 1. Schematic diagram of crazing device.

direction of the crazing-processing (shown by the direction of an arrow in Fig. 1) was adjusted to be perpendicular to the extrusion direction at the time of manufacturing of the PS film. All experiments were conducted at room temperature.

2.3. Measurements of crazes

Craze morphology in the sample was observed by an optical microscope, Width, interval and length of the crazes were defined as the length of the craze region in the crazing-processing direction, the length of the non-craze region in the crazing-processing direction and the length of the craze region perpendicular to the craze-processing direction, respectively. Those were measured using an optical measurement-microscope (Nikon Co., Measurescope MM-22). Over 50 samples were examined for each experimental condition.

2.4. Measurements of mechanical properties

Tensile strength and Young's modulus of the crazing-processed specimens were measured by a tensile tester in directions parallel and perpendicular to the crazing-processing direction. Test species (width, 10 mm; length, 50 mm) were tested with a gage length of 30 mm and a tensile rate of 10 mm/min.

2.5. Measurements of optical properties

The incident angle dependence of the transmittance was measured to estimate the view selectability of the crazed films. White light was used as the light source. The white light penetrated the sample cell on a rotating disk and was measured by a power meter (Nihon-kagaku Engineering Co., laser power meter PM-201) as shown in Fig. 2. The crazing-processing direction of the crazed film was fixed horizontally on a rotating disk.

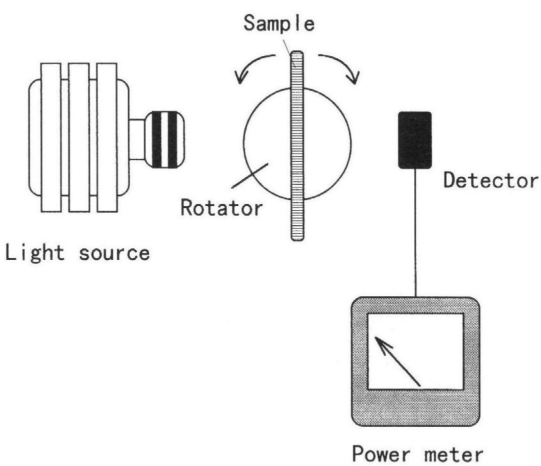

Figure 2. Schematic diagram of light scattering measuring instrument.

3. RESULTS AND DISCUSSION

3.1. Form of crazes

The formation of crazing regions is common to polymers. The structure of crazes is similar to a sponge composed of fibrils and voids, but quite different from cracks. Crazes exhibit elastic characteristics while maintaining tensile strength. In this paper, the modification of PS film, which is similar to a craze and a shear band, was considered as a craze. Figure 3 shows the photographs by transmitted light of a PS film after the crazing-processing. A horizontal direction in the pictures was the same as the direction of the crazing-processing. The craze region are seen as the black stripes perpendicular to the direction of the crazing-processing while the non-craze regions are seen as the white regions. This is because the incident light was scattered by voids in the crazes.

Crazes were generated uniformly by the crazing-processing. The craze fraction in the film increased with an increase in tension at the crazing-processing. The craze length was above 200 μm in comparison with *ca* 80 μm of the crazing-processed PVDF film at the standard conditions (the pulling rate of 10 mm/min, the crazing tension of 8 N/cm and the thickness of 25 μm).

Craze morphology of the film surface was observed by optical micrography of reflected light. The crazes were observed on either side of the crazed film in contact and non-contact with the crazing edge during the crazing-processing at the crazing tension of 6 N/cm. It is seen that crazes completely traverse the film. Gas permeability (nitrogen) of the crazed PS film increased with increasing craze fractions. The results

(a)

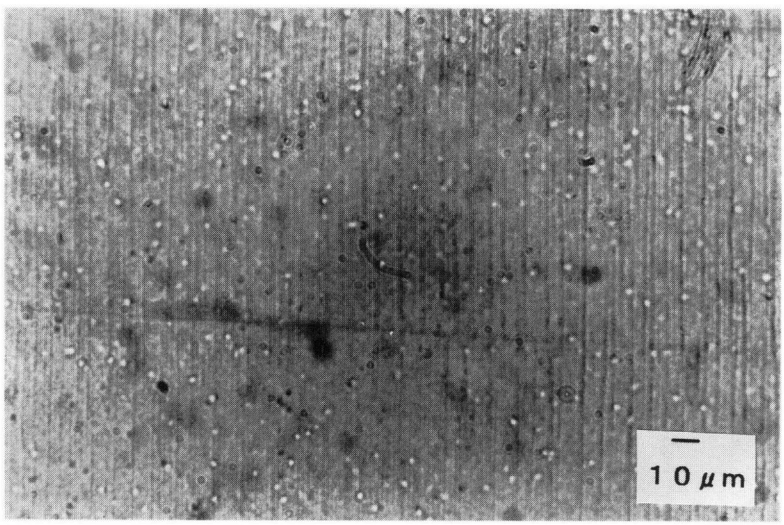

Figure 3. Optical micrographs of crazed PS: pulling rate, 10 mm/min; (a) tension 2 N/cm; (b) tension 6 N/cm.

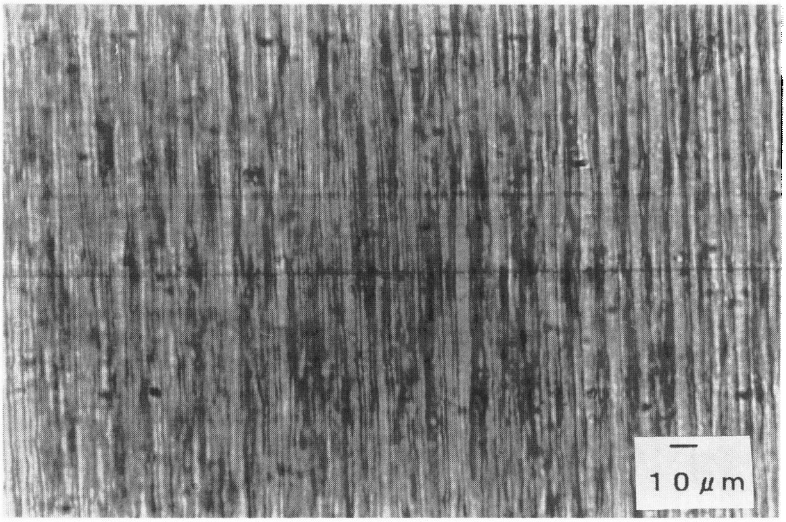

(b)

Figure 3. (Continued).

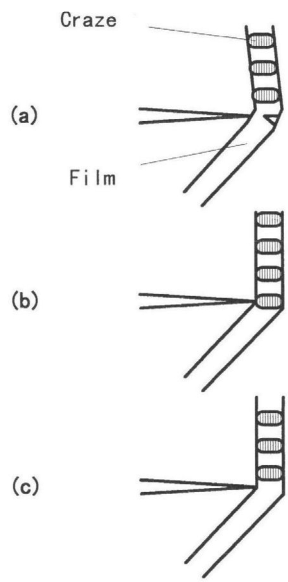

Figure 4. Schematic diagram of crazing-processing (cross-sectional view at crazing edge): (a) stress concentration; (b) crazing and released stress; (c) to next crazing.

of gas permeability measurement for the crazed film showed the craze regions went through the thickness of the film without any gradual film breakage. However, splits were found to be located at 0.03 – 0.04 μm from the surface by a cross-sectional view of the transmittance electron microscope pictures.

In the crazing-processing, the PS film was bent sharply and the stress was concentrated at the crazing edge as schematically shown in Fig. 4a. The craze in the film at the crazing edge is caused by stress without leading to fracture (Fig. 4b), because the concentrated stress was released at the same time as the generation of he crazes which had the lower Young's modulus and elastic properties as reported for a crazing PVDF in a previous paper [5]. The crazing edge had been shifted to a non-crazing region of the film according to the moving of the sample film (Fig. 4c). The stress would have been concentrated and the next craze would have grown in much the same manner as the previous craze, and crazes were caused periodically and continuously.

3.2. Width and interval of crazes

The width and interval of the crazes affected optical and mechanical properties of the crazing-processed film. Figure 5 indicates the width, interval and the sum of

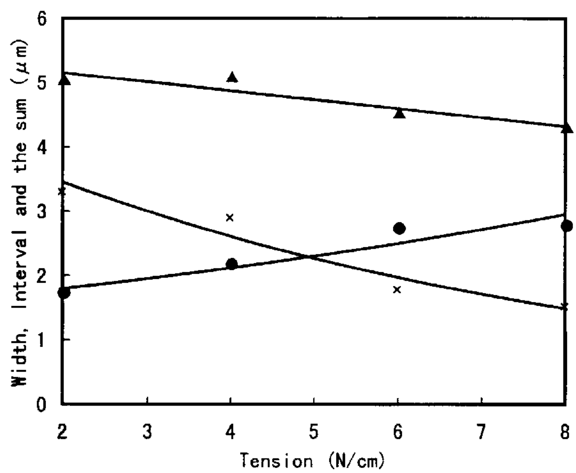

Figure 5. Crazing tension dependence of width (●), interval (×) and the sum (▲) for crazed PS film: pulling rate 10 mm/min.

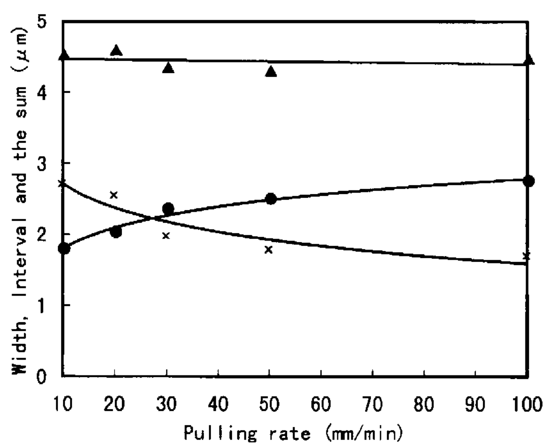

Figure 6. Pulling rate tension dependence of width (●), interval (×) and the sum (▲) for crazed PS film: tension 6 N/cm.

width and interval as a function of the tension during a crazing-processing under a constant pulling rate. The width of the crazes increased and the interval (i.e. the non-craze width) decreased with increasing tension. Increasing the width and narrowing of the interval induced an increase in the fraction of the crazes in the PS film. The sum of the width and interval indicated a craze repeating unit length. It decreased slightly with increasing tension, because of an increase in the width of the crazes and a concomitant decrease in the interval.

Figure 6 shows the relationship between the width, the interval of the crazes and the pulling rate of the crazing-processing. The craze of the PS film had a narrower width and a wider interval due to an increase in the pulling rate of the crazing-processing. It was conceivable that the crazes did not grow sufficiently because the pulling rate was too fast to produce crazes.

The molecular orientation of the film is an important factor in the crazing-processing as reported in a previous paper [5]. No crazes can be observed under any conditions of this experiment in the direction of the crazing-processing parallel to the molecular orientation of the PS film.

3.3. Mechanical properties of crazing-processed PS films

Crazing-processing tension dependence of tensile strength and Young's modulus of the crazing-processed films under a constant pulling rate are shown in Fig. 7. The results of this figure were examined in a direction parallel to the crazing-processing. The tensile strength was almost unchanged with an increase in crazing-processing tension. The tensile strength of the craze regions was almost the same as the strength of the unprocessed film. On the other hand, Young's modulus decreased with an increase in processing tension. Young's modulus of the craze region at 8 N/cm of the tension was *ca* 0.32 GPa, which was the craze fraction and Young's modulus of PS film expected.

Figure 8 shows the dependence of the tensile strength and Young's modulus on the crazing-processing pulling rate under a constant processing tension. When generating

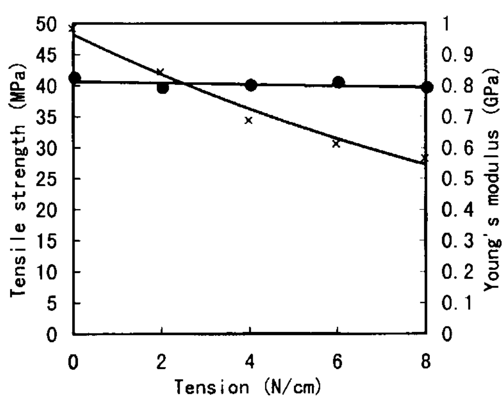

Figure 7. Crazing tension dependence of tensile strength (●) and Young's modulus (×) for crazed PS film: pulling rate 10 mm/min.

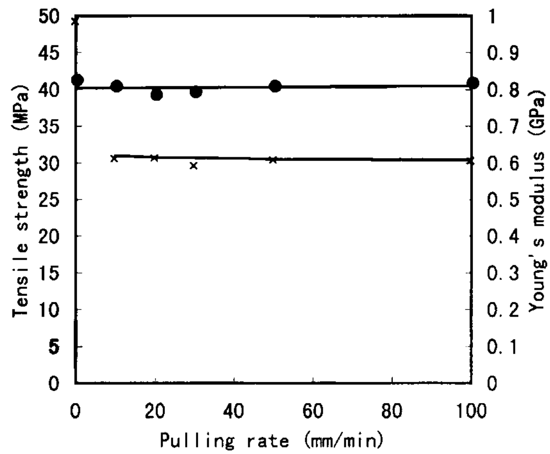

Figure 8. Pulling rate dependence of tensile strength (●) and Young's modulus (×) for crazed PS film: tension 6 N/cm.

a craze, Young's modulus decreases. However, the tensile strength and Young's modulus were almost unchanged with an increase in the pulling rate. The effect of pulling rate on the mechanical properties of the film was smaller than that of processing tension.

For practical uses of the crazed PS film, mechanical damage of crazing-processing will not be significant.

3.4. Optical properties of crazing-processed PS films

The change of optical transparency of the crazing-processed films result from the craze or the shear band creation. When the processing tension was strong, the scattering of incident light by voids in the crazes was efficient and the film appeared like frosted glass. By using a laser light scattering measuring instrument (IST Planning Co., SALS100G), a number of voids of submicron order could be observed. Incident light is generally scattered at random direction for crazed PS film by the conventional drawing-processing.

Under a constant pulling rate, incident angle dependence of optical transmittance as a function of processing tension is shown in Fig. 9. The angles of the incident light in a direction perpendicular to the film surface are zero degrees. Transmittance decreased in all incident angles when the crazing-processing tension increased: for example, it decreased from *ca* 90% at 4 N/cm to 40% at 6 N/cm at an incident angle of zero degrees. The steep decrease suggests the void in the craze would grow sufficiently for the incident light scattering from morphology resembling a shear band with a poor void. The shape of transmittance curve as a function of an incident angle was changed into a W-shape at a processing tension of 6 N/cm. Regarding a PS film displaying W-shape curve of transmittance (W-type transmittance), transparency decreased notably around the incident angle of 20 deg. The accuracy of the present curve is governed by the experimental error allowed for the unsymmetrical curve in this case.

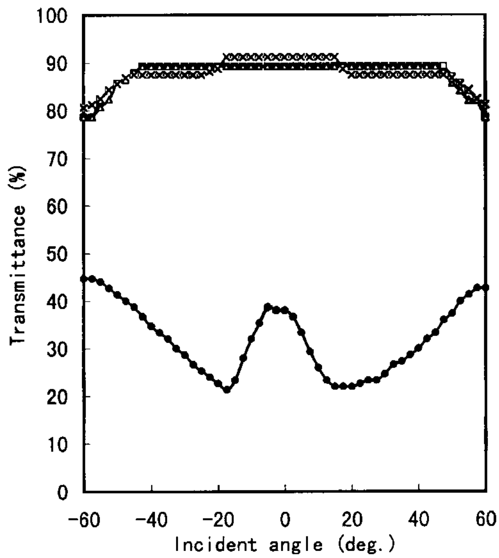

Figure 9. Incident angular dependence of transmittance for crazed PS films at various tension: pulling rate 10 mm/min; (□) PS film; (△) 2 N/cm; (×) 4 N/cm; (●) 6 N/cm.

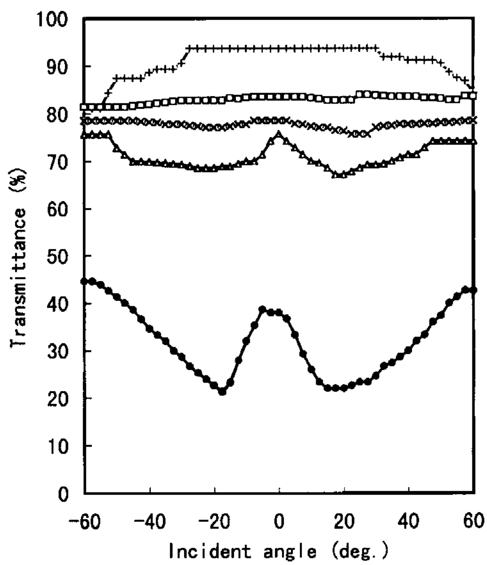

Figure 10. Incident angular dependence of transmittance for crazed PS films at various pulling rates: tension 6 N/cm; (+) PS film; (●) 10 mm/min; (△) 20 mm/min; (×) 30 mm/min; (□) 50 mm/min.

Figure 10 shows the relationship between incident angle and transmittance as a function of pulling rates under a constant processing tension. Under all incident angles, transmittance increased as the crazing-pulling rate increasing within a range of 10–50 mm/min: for example, it increased from 40% at 10 mm/min to about 85% at 50 mm/min at an incident angle of zero degrees. The width and interval of the craze

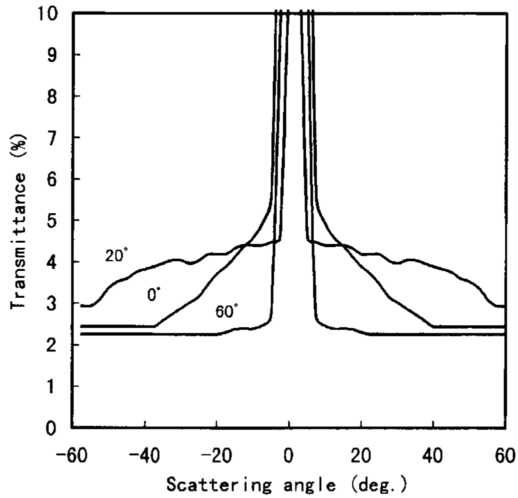

Figure 11. Scattering profiles of incident light for crazed PS film at incident angles of 0, 20 and 60 deg.

were 2.7 μm and 1.8 μm at 10 mm/min rates, 1.7 μm and 2.5 μm at 50 mm/min rates, respectively. The increasing of transmittance would be caused by the decreasing of the fraction of craze regions with the pulling rate increased. It was conceivable that in the case of a faster pulling rate, the crazes would not grow sufficiently and morphology resembling a shear band with a poor void developed. Also, when the pulling rate increased (over 30 mm/min), the characteristic of transmittance was changed from a W-shape to a flat profile. It was hypothesized that a lower pulling rate during crazing-processing would be the most suitable for inducing optimal growth of the craze regions.

Using the crazed PS film of a W-type transmittance, Fig. 11 shows the results of the incident light scattering measured at the incident angles of 0, 20 and 60 deg. The sample was fixed at each incident angle and the receiving part of the detector was moved (Fig. 2). At the incident angle of 20 deg, the scattered light diffused over a wide range. The scattered light was very weak at the incident angle of 60 deg compared to the incident angles of zero and 20 deg. The incident light scattering depended strongly on the angle of incident light. These scatterings of the crazed PS films would be created by the voids in the craze regions, and reflection and refraction between the craze and non-craze layers, geometrically. A more exact explanation takes into consideration that the dependence of wavelength is important.

The scattering of light by the crazes resulted in a decrease in trasmittance over the whole angle of incident light. The effect of scattering by the crazes will be weak because the incident light penetrates many craze layers at a wide incident angle; however, transmittance at the incident angle of 60 deg was higher.

Regarding the transmittance change that would be caused by the reflection between the craze and non-craze layers, we hypothesize that the non-craze layers act as an optical wave guide. Figure 12 shows the schematic diagram which is thought to be the reflection at the interface between the craze and non-craze layers. When the

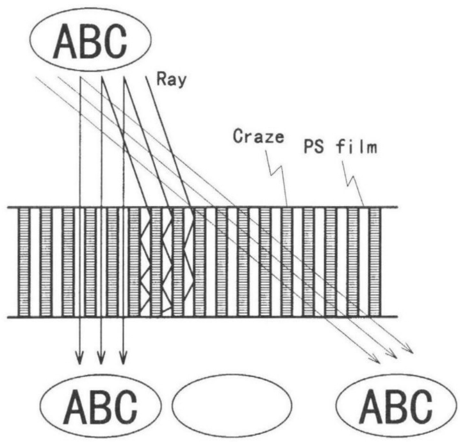

Figure 12. Schematic diagram of transmittance and reflection in crazing-processing PS film (cross-sectional view).

light entered perpendicularly to the film, transmittance was high (semi-transparency); however, when the incident light had a tilt angle, transmittance decreased because the direction of the light changed along the optical wave guide of non-craze layers (low-transparency). When the incident light had a wider tilt angle, the transmittance rose again, because the craze regions no longer functioned as an optical wave guide (transparency). This led to transmittance becoming a W-type.

That the light incident on the craze regions was scattered completely irrespective of the angle of incidence was remarkable. The craze layers acted like the slat of a blind. PVDF film after crazing-processing displayed maximum light transmittance at an incident angle of zero degrees and decreased with increasing incident angles (a Λ-type shape of transmittance curve) [5]. However, these simple ideas of optical anisotropy would not result in the all crazing-processing films, i.e. the width and the interval of the crazes were narrower than the wave length of the incident light.

4. CONCLUSIONS

By pulling PS film through a process with a sharp-edge bending under constant tension, many crazes penetrated the film in the thickness direction, being generated uniformly and regularly. These crazing-processed PS films were mono-component composites, which were composited with different high-order structures of a craze layer with a non-craze layer. In a previous paper [2], the crazing-processed PVDF films were transparent at the view angle of zero degrees and opaque at view angles above 30 deg. In this paper, the PS film processed under suitable conditions indicated a W-shape of light transmittance curve according to the incident angle. The transparency of the crazing-processed PS film was minimum at view angles of *ca* 20 deg. These anisotropic transparencies could be applied to create a view field selectable film.

REFERENCES

1. Maeda, K., Ishizuka, S., Tsujino, T., Yamamoto, H. and Takigawa, A. Optical performance of angle dependent light control glass. In: *SPIE Proc. 1536: Optical Materials Techology for Energy Efficiency and Solar Energy Conversion X* (1991), pp. 138–148.
2. Takeno, A., Furuse, Y., Miwa, M. and Watanabe, A. Anisotropic light scattering of crazed polymer film. *Sen-i Gakkai Preprints* **5**, 195 (1992).
3. Jpn Pat. H06-82607 (1994).
4. Tsuzuki, H., Takeno, A., Watanabe, A. and Miwa, M. Application of PVDF film by the crazing method. In: *24th Annual Meeting of Union of Chemistry-Related Societies in Chubu Area Jap. Preprint*. Gifu (1993), p. 371.
5. Takeno, A., Furuse, Y., Miwa, M. and Watanabe, A. Mono-component poly(vinylidene fluoride) composites by craze structural control. *Adv. Composite Mater.* **4**, 129–144 (1994).